Carnegie Observatories Astrophysics Series, Vol. 3:
Clusters of Galaxies: Probes of Cosmological Structure and Galaxy Evolution, 2004
ed. J. S. Mulchaey, A. Dressler, and A. Oemler (Cambridge: Cambridge Univ. Press)

Clusters of Galaxies in the Sloan Digital Sky Survey

ROBERT C. NICHOL
Department of Physics, Carnegie Mellon University

Abstract

I review here past and present research on clusters and groups of galaxies within the Sloan Digital Sky Survey (SDSS). I begin with a short review of the SDSS and efforts to find clusters of galaxies using both the photometric and spectroscopic SDSS data. In particular, I discuss the C4 algorithm, which is designed to search for clusters and groups within a seven-dimensional (7-D) data space, i.e., simultaneous clustering in both color and space. The C4 catalog has a well-quantified selection function based on mock SDSS galaxy catalogs constructed from the Hubble Volume simulation. These simulations indicate that the C4 catalog is $> 90\%$ complete, with $< 10\%$ contamination, for halos of $M_{200} > 10^{14} M_{\odot}$ at $z < 0.14$. Furthermore, the observed summed r-band luminosity of C4 clusters is linearly related to M_{200}, with $< 30\%$ scatter at any given halo mass. I also briefly review the selection and observation of luminous red galaxies and demonstrate that these galaxies have a similar clustering strength as clusters and groups of galaxies. I outline a new collaboration planning to obtain redshifts for 10,000 luminous red galaxies at $0.4 < z < 0.7$ using the SDSS photometric data and the Anglo-Australian Telescope 2dF instrument. Finally, I review the role of clusters and groups of galaxies in the study of galaxy properties as a function of environment. In particular, I discuss the "star formation rate-density" and "morphology-radius" relations for the SDSS and note that both of these relationships have a *critical density* (or "break") at a projected local galaxy density of $\sim 1\,h_{75}^{-2}\,\mathrm{Mpc}^{-2}$ (or between 1 to 2 virial radii). One possible physical mechanism to explain this observed critical density is the stripping of warm gas from the halos of infalling spiral galaxies, thus leading to a slow strangulation of star formation in these galaxies. This scenario is consistent with the recent discovery (within the SDSS) of an excess of "passive" or "anemic" spiral galaxies located within the infall regions of C4 clusters.

1.1 Introduction

As demonstrated by this conference—*Clusters of Galaxies: Probes of Cosmological Structure and Galaxy Evolution*—clusters and groups of galaxies have a long history as key tracers of the large-scale structure in the Universe and as laboratories within which to study the physics of galaxy evolution. At the conference, their important role as cosmological probes was reviewed by several speakers, including Gus Evrard and Alan Dressler. Therefore, I will not dwell on justifying the importance of clusters to cosmological research, but simply direct the reader to the reviews by these authors.

Instead, I provide below a brief overview of the Sloan Digital Sky Survey (SDSS), followed by a discussion of the cluster-finding algorithms (§1.2) used within the SDSS collaboration, and present new scientific results obtained from studies of galaxies as a function of environment (§1.5).

1.1.1 The Sloan Digital Sky Survey

The SDSS (York et al. 2000; Stoughton et al. 2002) is a joint multicolor (u, g, r, i, z) imaging and medium resolution (R = 1800; 3700 to 9100 Å) spectroscopic survey of the northern hemisphere using a dedicated 2.5 meter telescope located at the Apache Point Observatory near Sunspot, New Mexico. During well-defined (seeing $<1\farcs7$) photometric conditions, the SDSS employs a mosaic camera of 54 CCD chips to image the sky via the drift-scanning technique (see Gunn et al. 1998). These data are reduced at Fermilab using a dedicated photometric analysis pipeline (PHOTO; see Lupton et al. 2001), and object catalogs are obtained for spectroscopic target selection. During nonphotometric conditions, the SDSS performs multiobject spectroscopy using two bench spectrographs attached to the SDSS telescope and fed with 640 optical fibers. The other ends of these fibers are plugged into a pre-drilled aluminum plate that is bent to follow the 3-degree focal surface of the SDSS telescope. The reader is referred to Smith et al. (2002), Blanton et al. (2003), and Pier et al. (2003) for more details about the SDSS.

In this way, the SDSS plans to image the northern sky in five passbands, as well as obtain spectra for $\sim 10^6$ objects. In addition to the large amount of the data being collected, the quality of the SDSS data is high, which is important for many of the scientific goals of the survey. For example, the SDSS has a dedicated photometric telescope (Hogg et al. 2001), which is designed to provide the SDSS with a global photometric calibration of a few percent accuracy over the whole imaging survey. Also, SDSS spectra are spectrophotometrically calibrated.

The SDSS is now in production mode and has been collecting data for several years. As of January 2003, the SDSS had obtained 4470 deg^2 of imaging data (not unique area) and had measured a half million spectra. The SDSS has just announced its first official data release (see `http://www.sdss.org/dr1/`).

1.2 SDSS Cluster Catalogs

One of the fundamental science goals of the SDSS was to create new catalogs of clusters from both the imaging and spectroscopic data. In Table 1.1, I present a brief overview of past and present efforts within the SDSS collaboration as part of the SDSS Cluster Working Group. In this table, I provide an appropriate reference if available, a brief description of the cluster-finding algorithm, and the SDSS data being used to find clusters. Each of these algorithms has different strengthens and science goals, and a detailed knowledge of their selection functions is required before a fair comparison can be carried out between these different catalogs. The reader is referred to the review of Postman (2002) for more discussion of this point. However, Bahcall et al. (2003) have begun this process by performing a detailed comparison of the clusters found by both the AMF and maxBCG algorithms. The product of this work is a joint catalog of 799 clusters in the redshift range $0.05 < z < 0.3$ selected from ~ 400 deg^2 of early SDSS commissioning data.

As first outlined in Nichol et al. (2001), there are four main challenges to producing a robust, optically selected catalog of clusters. These are:

Table 1.1. *Overview of past and present efforts to find clusters and groups of galaxies within the SDSS collaboration. In the data column, "I" is for SDSS imaging data and "S" is for SDSS spectral data.*

Name	Reference	Data	Description
maxBCG	Annis et al. (2004)	I	Model colors of brightest cluster galaxies with z and look for E/S0 ridge-line
AMF	Kim et al. (2002)	I	Matched-filter algorithm looking for overdensities in luminosity and space
CE	Goto et al. (2002)	I	Color cuts, then uses SEXTRACTOR to find and deblend clusters
F-O-F	Berlind et al. (2004)	S	Friends-of-friends algorithm
Groups	Lee et al. (2004)	I	Mimics Hickson groups criteria
BH	Bahcall et al. (2003)	I	Merger of maxBCG and AMF
C4	Nichol et al. (2001)	I + S	Simultaneous clustering of galaxies in color and space

(1) To eliminate projection effects. This problem has plagued previous catalogs of clusters and has been discussed by many authors (see, for example, Lucey et al. 1983; Sutherland 1988; Nichol et al. 1992; Postman, Huchra, & Geller 1992; Miller 2000).

(2) A full understanding of the selection function. This has been traditionally ignored for optical cluster catalogs (see Bramel, Nichol, & Pope 2000; Kochanek et al. 2003), but is critical for all statistical analyses using the catalog.

(3) To provide a robust mass estimator. Traditionally, this has been the Achilles' Heel of optical catalogs, as richness is a poor indicator of mass.

(4) To cover a large dynamic range in both redshift and mass.

I review below one SDSS cluster catalog with which I am involved in collaboration with Chris Miller at Carnegie Mellon University, which now meets these four challenges and is comparable in quality to the best X-ray catalogs of clusters (e.g., the REFLEX catalog of Böhringer et al. 2001).

1.3 The C4 Algorithm

The underlying hypothesis of the C4 algorithm is that a cluster or group of galaxies is a clustering of galaxies in both color and space. This is demonstrated in Figure 1.1, and the reader is referred to Gladders & Yee (2000) for a full discuss of all the evidence in support of this hypothesis. Therefore, by searching for clusters simultaneously in both color and space, the C4 algorithm reduces projection effects to almost zero, while still retaining much power for finding clusters (see Fig. 1.2).

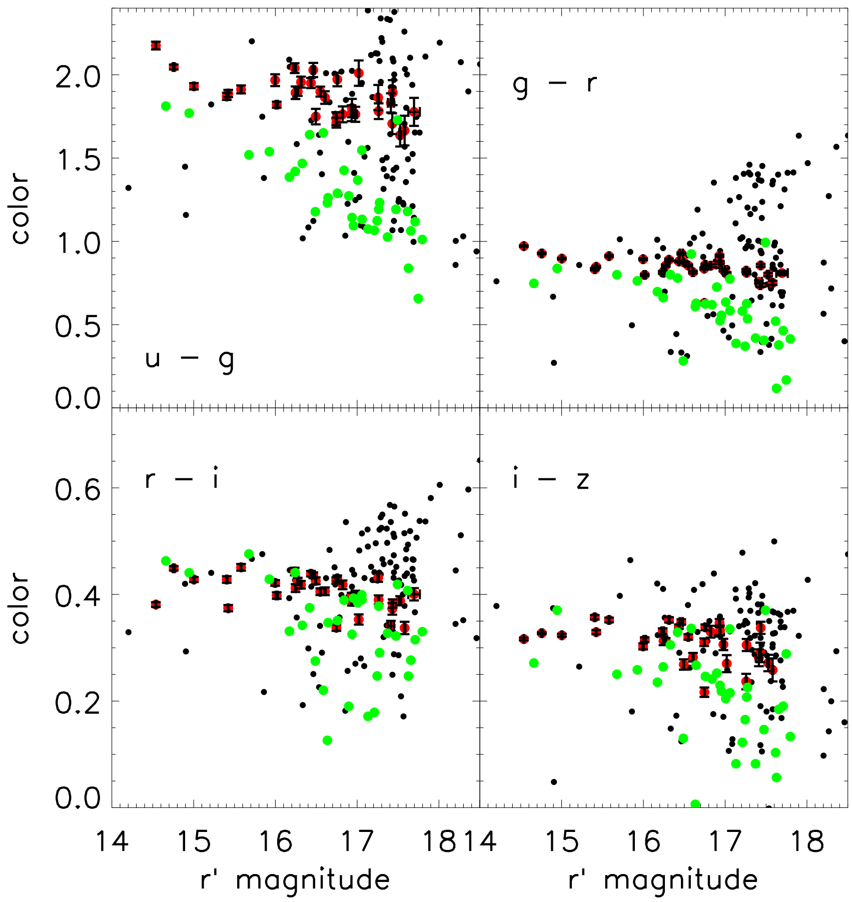

Fig. 1.1. The color-magnitude relations for a previously undiscovered $z = 0.06$ cluster in the Early Data Release of the SDSS detected by the C4 algorithm. The black dots are galaxies within an aperture of $1h^{-1}$ Mpc around the cluster center. Note the tight correlation in color of the points with error bars, which is the E/S0 ridge-line and is the signal the C4 algorithm uses to find clusters.

1.3.1 Overview of C4 Algorithm

I present here a brief overview of the C4 algorithm. To date, the C4 algorithm has been applied to the SDSS main galaxy spectroscopic sample (Strauss et al. 2002) in the Early Data Release of the SDSS (see Stoughton et al. 2002; Gómez et al. 2003).

For each galaxy in the sample—called the "target" galaxy below—the C4 algorithm is performed in the following steps.

(1) A 7-D rectangular box is placed on the target galaxy. The center of this box is defined by the observed photometric colors (i.e., $u-g$, $g-r$, $r-i$, $i-z$), the Right Ascension, Declination, and redshift of the target galaxy. The width of the box is dependent on the redshift and

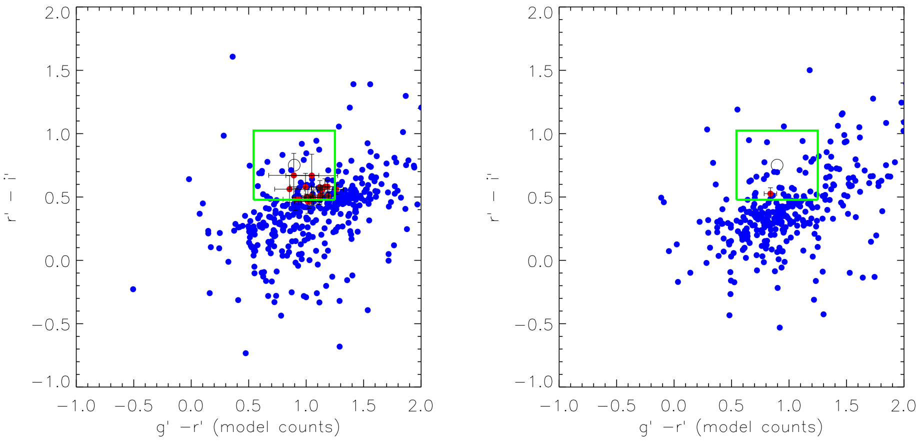

Fig. 1.2. Color-color plots for a sample cluster galaxy (*left*) and a randomly chosen field position (*right*). The black dots are all galaxies within the spatial part of the 7-D search box centered on the target galaxy (i.e., all galaxies satisfying the R.A., Dec., and z dimensions of the 7-D box). The points with error bars are now those galaxies which also lie within the color part of the 7-D search box; i.e., they are close in both space and color. The box is the size of the 7-D box in this color-color plane, and is much smaller than the scatter seen in the black points. For the random field position, there is only one point with an error bar inside the box compared to 10 around the cluster galaxy. Therefore, all projection effects have been eradicated as one does not expect false clustering in such a high-dimensional space.

photometric errors on the colors of the target galaxy. Once the box is defined, the number of neighboring galaxies is counted within the SDSS main galaxy sample (Strauss et al. 2002) inside this box, and this count is reported (see Fig. 1.2).

(2) The same 7-D box is placed on 100 randomly chosen galaxies, also taken from the SDSS main galaxy spectroscopic sample, that possess similar seeing and reddening values (see Fig. 1.2). For each of these 100 randomly chosen galaxies, the number of neighboring galaxies is counted (from the SDSS main galaxy sample) inside the box and a distribution of galaxy counts is constructed from these 100 randomly chosen galaxies.

(3) Using this observed distribution of galaxy counts, the probability of obtaining the observed galaxy count around the original target galaxy is computed.

(4) This exercise is repeated for all galaxies in the sample, and then all these probabilities are ranked.

(5) Using the "false discovery rate" (Miller et al. 2001) with an $\alpha = 0.2$ (i.e., only allowing a false discovery rate of 20%), a threshold in probability is determined that corresponds to galaxies that possess a high count of nearest neighbors in their 7-D box.

(6) All galaxies in our sample below this threshold in probability are removed, which results in the eradication of $\sim 80\%$ of all galaxies. By design, the galaxies that are removed are preferentially in low-density regions of this 7-D space (i.e., the field population). The galaxies that remain are called "C4 galaxies," which, by design, reside in high-density regions with neighboring galaxies that possess the same colors as the target galaxy. Figure 1.3 illustrates this step.

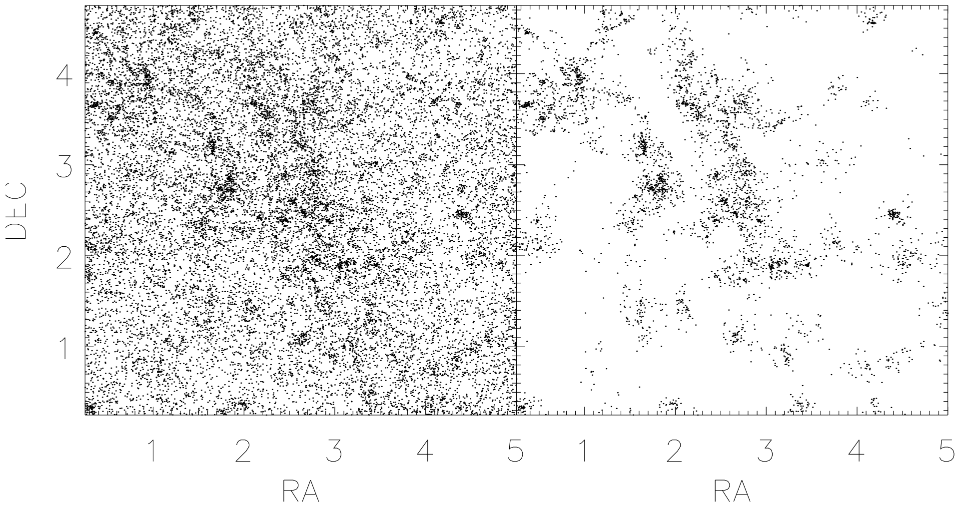

Fig. 1.3. The projected galaxy distribution in the simulations before (*left*) and after (*right*) the C4 algorithm has been run and a threshold applied to eliminate field-like galaxies. This illustrates the effect of step 6 in the algorithm.

(7) Using only the C4 galaxies, the local density of all the C4 galaxies is determined using the distance to the 10^{th} nearest neighbor.
(8) The galaxies are rank ordered based on these measured densities and then assigned to clusters based on this ranked list. This is the same methodology as used to create halo catalogs within *N*-body simulations (see Evrard et al. 2002).
(9) This results in a list of clusters, for which a summed total optical luminosity (z and r bands) and a velocity dispersion are computed (see below).

In summary, the C4 algorithm is a semi-parametric implementation of adaptive kernel density estimation. The key difference with this approach, compared to previous cluster-finding algorithms, is that it does not model either the colors of cluster ellipticals (e.g., Gladders & Yee 2000; Goto et al. 2003) or the properties of the clusters (e.g., Postman et al. 1996; Kepner et al. 1999; Kim et al. 2002). Instead, the C4 algorithm only demands that the colors of nearby galaxies are the same as the target galaxy. In this way, the C4 algorithm is sensitive to a diverse range of clusters and groups; for example, it would detect a cluster dominated by a extremely "blue" population of galaxies (compared to the colors of field galaxies).

1.3.2 Simulations of the SDSS Data

To address the four challenges given above, it is vital that we construct realistic simulations of the C4 cluster catalog. This has now been achieved through collaboration with Risa Wechsler, Gus Evrard, and Tim McKay at the University of Michigan. Briefly, mock SDSS galaxy catalogs have been created using the dark matter distribution from the Hubble Volume* simulations (Evrard et al 2002). The procedure for populating the dark

* http://www.mpa-garching.mpg.de/Virgo/hubble.html

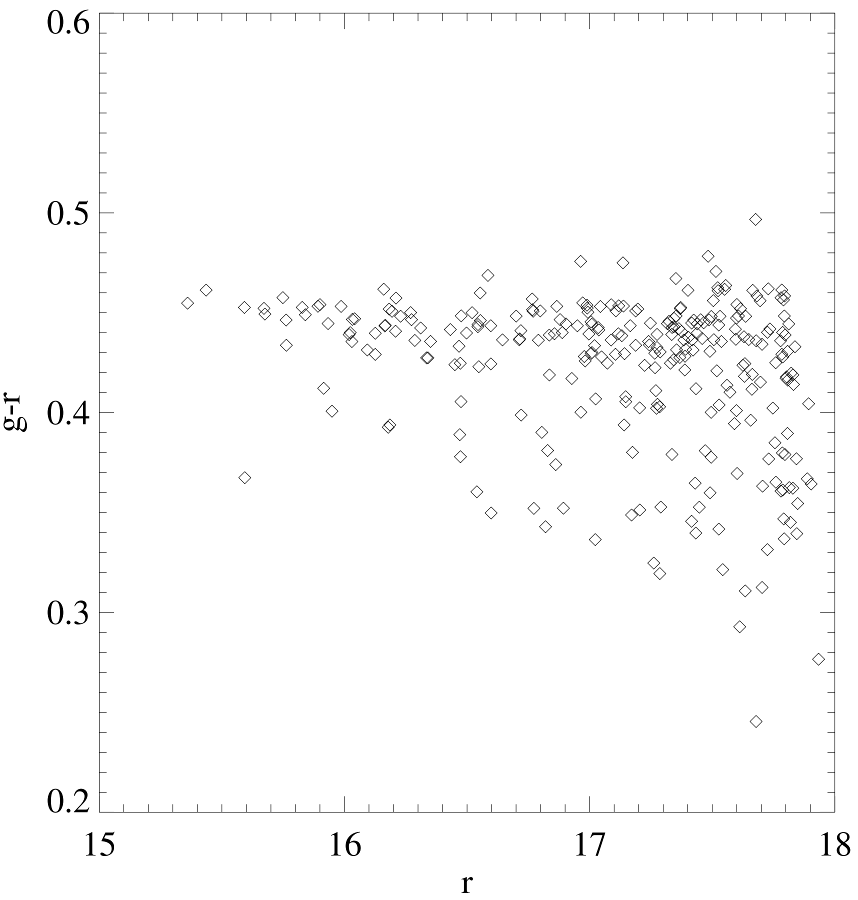

Fig. 1.4. The color-magnitude relations for a $z = 0.06$, $10^{15} M_\odot$ halo in the Hubble Volume simulation, where galaxies with SDSS colors and luminosities have been added to the simulation.

matter distribution with galaxies is described in detail by Wechsler et al. (2004), but I present a brief overview here. The simulation we use provides the dark matter distribution of the full sky out to $z \approx 0.6$, where the dark matter clustering is computed within the light cone. Galaxies, with r-band luminosities following the luminosity function found by Blanton et al (2001) for the SDSS, are added to the simulation by choosing simulation particles (with mass $\sim 2.2 \times 10^{12} M_\odot$ per particle) from a probability density function of local mass density that depends on galaxy luminosity. This luminosity-dependent probability density function is tuned so that the resulting galaxies match the luminosity-dependent two-point correlation function (Zehavi et al. 2002). Colors are then added to the simulation using the colors of actual SDSS galaxies with similar luminosities and local galaxy densities. The resulting

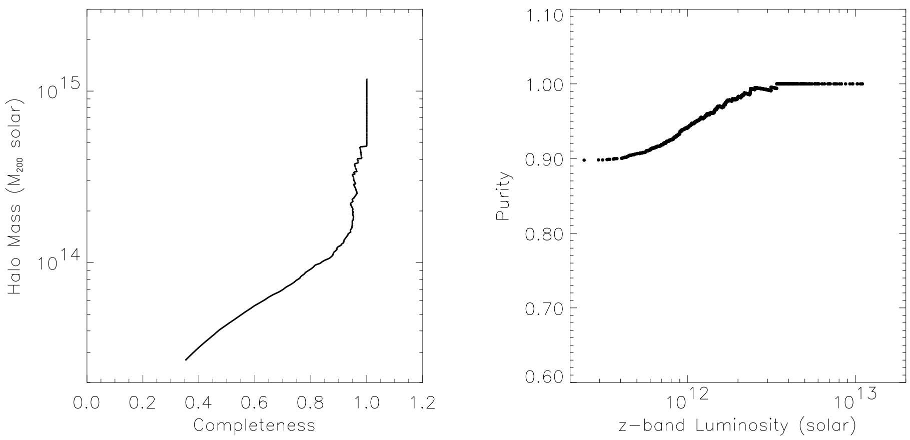

Fig. 1.5. *Left*: The completeness of the C4 catalog as a function of the dark matter halo mass (M_{200}) from the simulation. *Right*: The purity of the C4 catalog as a function of the summed total *r*-band luminosity of the cluster, as derived from our mock SDSS galaxy catalog.

catalog thus matches the luminosity function and color- and luminosity-dependent two-point correlation function of the SDSS data.

Therefore, these mock SDSS catalogs produce clusters of galaxies with a realistic color-magnitude diagram (compare Figs. 1.1 and 1.4). As we know the location of all the massive halos (i.e., the clusters) within the Hubble Volume simulation (see Jenkins et al. 2001 and Evrard et al. 2002), we can now use these mock catalogs to derive the selection function of the C4 algorithm. The benefit of this approach is that these mock catalogs contain realistic projection effects, as the galaxy clustering is constrained to match the real data, and the clusters (halos) possess realistic profiles, ellipticities, and morphologies. This is a significant advancement compared to past simulations used to quantify the selection function of cluster catalogs (see Postman et al. 1996; Bramel et al. 2000; Goto et al. 2002).

For comparison between the real and simulated data, two different cluster observables are used. The first is the bi-weighted velocity dispersion, and the second is the summed optical luminosity of the galaxies within the cluster. To calculate the velocity dispersion (σ_v), an iterative technique is performed using the robust bi-weighted statistics of Beers, Flynn, & Gebhardt (1990). The total optical luminosity of the clusters is determined by converting the apparent magnitudes of galaxies in the cluster to optical luminosities using the conversions in Fukugita et al. (1996). All magnitudes are also *k*-corrected according to Blanton et al. (2002) and extinction corrected according to Schlegel, Finkbeiner, & Davis (1998). Cluster membership is defined to be any galaxy within $4\sigma_v$ in redshift and within $1.5h^{-1}$ Mpc projected separation on the sky. For the halo catalog, the mass within 200 times the critical density (M_{200}), as determined from summing up all the dark matter particles within this radius around each halo (R_{200}; see Evrard et al. 2002), is used.

1.3.3 Purity and Completeness: Challenges One and Two

The C4 algorithm has been applied to these mock SDSS galaxy catalogs. In Figure 1.5, I show the purity of the matched C4 clusters found in the simulation as a function of the total r-band luminosity. Purity is defined to be the percentage of systems detected in the mock SDSS catalog, using the C4 algorithm, that match a known dark matter halo in the Hubble Volume simulation. Clearly, the purity of the C4 catalog remains high over nearly 2 orders of magnitude in luminosity and is a direct result of searching for clustering in a high-dimensional space where projection effects are rare.

In Figure 1.5, I also present the completeness of the C4 catalog, as a function of the dark halo mass (M_{200}), and demonstrate that the C4 catalog remains $> 90\%$ complete for systems with $M_{200} > 10^{14} M_{\odot}$. The accuracy of these completeness measurements greatly benefits from the large sample sizes available from the Hubble Volume simulation. However, for the lower-mass systems, there may be some incompletenesses in the original dark matter halo catalog because of the mass resolution of the Hubble Volume simulations. Furthermore, the purity and completeness of the C4 catalog are only a weak function of the input parameters (e.g., the false discovery rate threshold) and thus are robust against the exact parameter choices. In summary, using these mock SDSS catalogs, we have addressed the first two challenges given in §1.2: for $z < 0.14$ and halos of $M_{200} > 10^{14} M_{\odot}$, the C4 catalog is $> 90\%$ complete, with $< 10\%$ contamination.

1.3.4 Mass Estimator and Dynamic Range: Challenges Three and Four

In Figure 1.6, I present the correlation between the M_{200} dark matter halo mass (taken directly from Evrard et al. 2002) and the total summed r-band luminosities for 4734 clusters that match in the Hubble Volume simulation. As expected, these two quantities are linearly correlated over 2 orders of magnitude in both the halo mass and optical luminosity. The measured scatter for the whole data set is 25% (measured perpendicular to the best-fit line). This plot demonstrates that we have address the third and fourth challenges in §1.2.

In the future, the C4 algorithm will be extended to include: (1) higher-resolution dark matter simulations to test the sensitivity of the algorithm to lower-mass systems, (2) a range of cosmological simulations to probe our sensitivity to various cosmological parameters (e.g., σ_8), and (3) improved methods of populating the simulations with SDSS galaxies using higher-order statistics (e.g., the three-point correlation function).

1.4 Luminous Red Galaxies

I briefly review here forthcoming surveys of luminous red galaxies (LRGs), as these surveys will soon replace clusters as the most efficient tracers of the large-scale structure in the Universe. Such galaxies are selected to be dominated by an old stellar population (using the SDSS colors) and are luminous, so they can be seen to high redshift even in the SDSS photometric data (see Eisenstein et al. 2001 for details).

A preliminary analysis of the correlation functions for both a sample of LRGs, selected from the SDSS (Eisenstein et al. 2001), and normal SDSS galaxies (Zehavi et al. 2001) demonstrates that, as expected, the LRGs are more strongly clustered than normal galaxies. The LRG correlation function has an amplitude and scale length consistent with that measured for groups and clusters of galaxies (e.g., Peacock & Nicholson 1991; Nichol et al. 1992; Collins et al. 2000; Miller 2000; Nichol 2002). Therefore, by design, a large fraction of these LRGs must lie in dense environments, as their spatial distribution clearly traces the

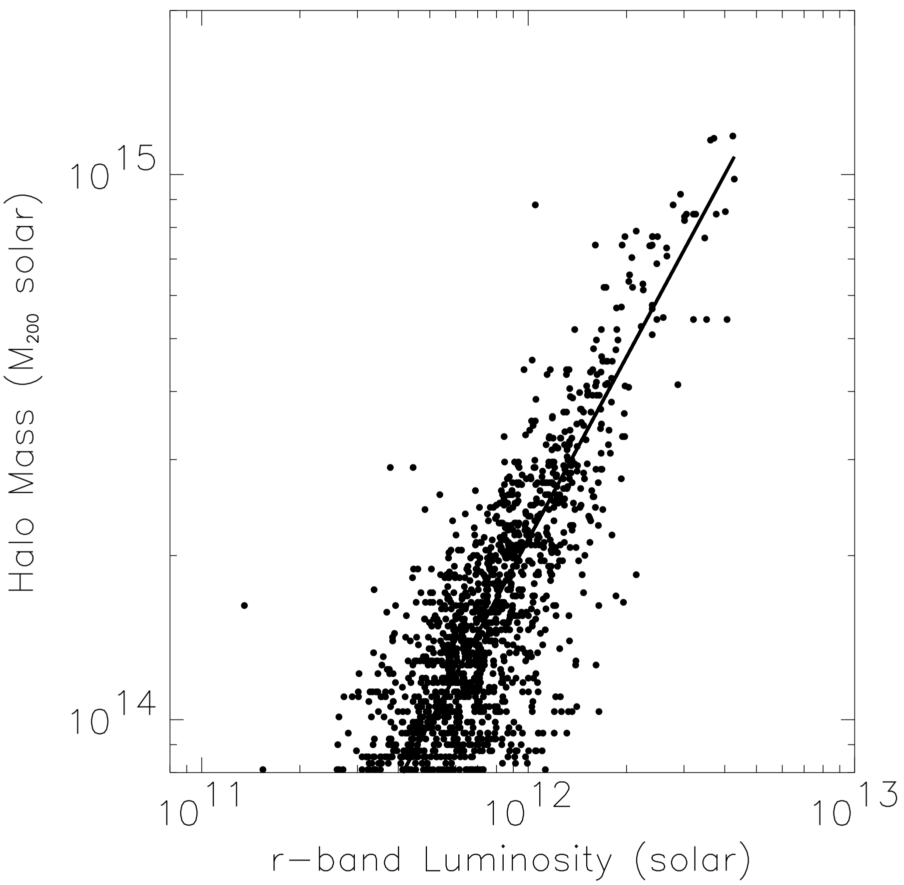

Fig. 1.6. The relation between the dark matter halo mass in our simulation and the total summed r luminosity. The line is the best fit, and the scatter, for a given mass, is $< 30\%$.

distribution of clusters and groups in the Universe. The main advantage of the LRG selection is that it does not depend upon the details of finding clusters of galaxies, and, therefore, their selection is more straightforward to model (see Eisenstein et al. 2001).

Due to the 45 minute spectroscopic exposure time of the SDSS, the SDSS only targets LRG candidates brighter than $r = 19.5$ mag (Eisenstein et al. 2001). This corresponds to a cut-off at $z \simeq 0.45$, but one can easily detect LRG candidates in the SDSS photometric data to higher redshifts.* Therefore, using the unique 2dF multiobject spectrograph on the Anglo-Australian Telescope, we have begun a joint SDSS-2dF program to push the original SDSS LRG selection to higher redshift. At the time of writing, our initial observations have been very successful, with spectra for ~ 1000 LRGs in the redshift range of $0.4 < z < 0.7$. In

* Beyond $z = 0.45$, the SDSS LRG selection becomes easier than at lower redshift (with less contamination) because of the fortuitous design of the SDSS filter system (see Eisenstein et al. 2001).

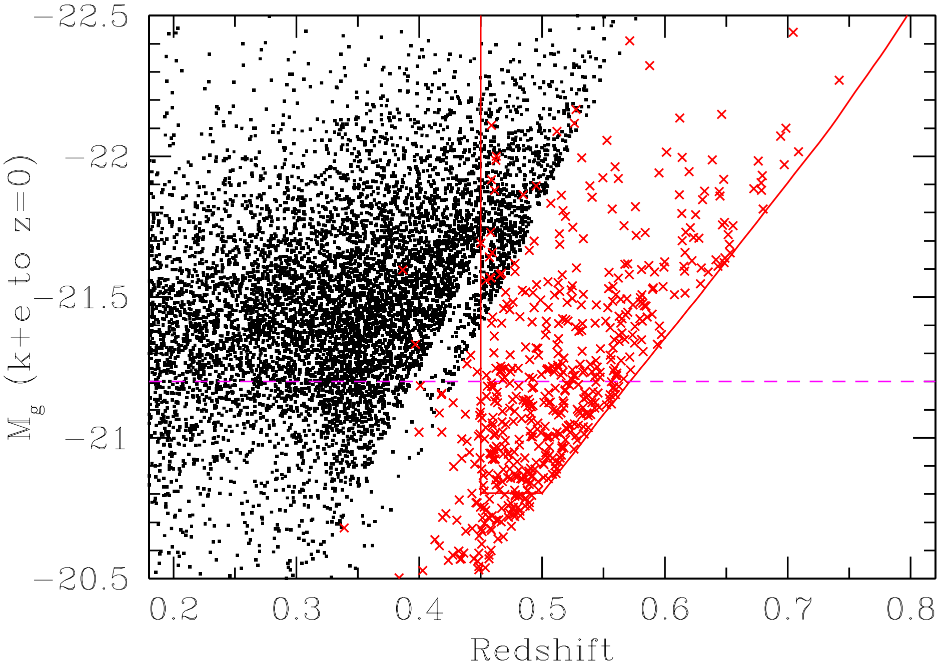

Fig. 1.7. The distribution in *g*-band luminosity and redshift for both the low-redshift LRGs (solid points) and the SDSS-2dF LRGs (crosses). The luminosities are *k*-corrected and corrected for passive evolution to $z = 0$. The solid lines show the expected selection boundaries for the SDSS-2dF survey, while the dashed line is the luminosity limit above which we expect the low-redshift SDSS LRG sample to be complete. Plot courtesy of Daniel Eisenstein and my SDSS-2dF colleagues.

Figure 1.7, I show the distribution in luminosity and redshift of these new SDSS-2dF LRGs and highlight that they cover a comparable range in their luminosities as the low-redshift LRGs. By the end of the SDSS-2dF LRG survey, we hope to have redshifts for 10,000 LRGs over this intermediate-redshift range. When combined with the low-redshift SDSS LRGs, we will be able to study the evolution in the properties and clustering of a single population of massive galaxies over half the age of the Universe.

1.5 Galaxy Properties as a Function of Environment

Clusters and groups of galaxies play an important role in studying the effects of environment on the properties of galaxies. With the SDSS data, it is now possible to extend such studies well beyond the cores of clusters into lower-density environments. Furthermore, the distance to the N^{th} nearest neighbor can be used to provide an adaptive measure of the local density of galaxies (see Dressler 1980; Lewis et al. 2002; Gómez et al. 2003). One can also use kernel density estimators (e.g., Eisenstein 2003).

There were many great talks and posters on the topic of galaxy evolution in clusters at this conference. For example, see the contributions by Bower, Davies, Dressler, Franx, Goto, Martini, N. Miller, Poggianti, Tran, and Treu. Also, I refer the reader to the work of Hogg et al. (2003), who is also using the SDSS data to study the effects of environment on the colors, surface brightnesses, morphologies, and luminosities of galaxies.

1.5.1 Critical Density

Is the star formation rate (SFR) of a galaxy affected by its environment? The answer appears to be yes, and was discussed by several authors at this conference. In particular, Gómez et al. (2003) find that the fraction of strongly star-forming galaxies in the SDSS decreases rapidly beyond a critical density of $\sim 1\,h_{75}^{-2}\,\mathrm{Mpc}^{-2}$ (see also Lewis et al. 2002). This result is demonstrated in Figure 1.8 and appears to be the same for all morphological types (see Gómez et al. 2003 and below).

In Figure 1.9, we also show a preliminary SDSS *morphology-radius* relation based on the work of Goto et al. (2004). The morphological classifications used in this figure are based on the new and improved concentration index C_{in} (see Shimasaku et al. 2001) measurements of Yamauchi et al. (2004). Briefly, Yamauchi et al. compute their concentration index within two-dimensional, elliptical isotopes, which account for the observed ellipticity and orientation of the galaxy on the sky. This improvement helps prevent low-inclination galaxies (e.g., edge-on spirals) from being misclassified as early-type galaxies. Furthermore, Yamauchi et al. computes the “coarseness” of each galaxy, which is a measure of the residual variance after the best-fit two-dimensional galaxy model has been subtracted. This coarseness measurement can therefore detect the presence of spiral arms in a galaxy. These two measurements of the morphology are re-normalized (by their rms) and added to produce a final morphological parameter called T_{auto} . Yamauchi et al. have tested their algorithm extensively and have demonstrated that T_{auto} is more strongly correlated with visual morphological classifications than the normal C_{in} parameter, with a correlation coefficient with the visual morphologies of 0.89.

Using the T_{auto} classification, Goto et al. (2004) have separated SDSS galaxies into the four (traditional) morphological subsamples of ellipticals, lenticulars (S0s), early-type (Sa and Sb) spirals and late-type systems (Sc spirals and irregulars). This is presented in Figure 1.9. Clearly, the mapping between the T_{auto} parameter and these visually derived morphological classifications is not perfect, but such an analysis does allow for an easier comparison with previous measurements of the morphology-radius and morphology-density relations, and theoretical predictions of these relationships (see Benson et al. 2000).

The SDSS morphology-radius relation shown in Figure 1.9 remains constant at > 2 virial radii from C4 clusters. As expected, this corresponds to low-density regions ($< 1\,h_{75}^{-2}\,\mathrm{Mpc}^{-2}$) in our volume-limited sample. This observation is consistent with previous determinations of the morphology-density and morphology-radius relations in that these functions are nearly constant at low densities (see Dressler 1980; Postman & Geller 1984; Dressler et al. 1997; Treu et al. 2003). At a radius of ~ 1 virial radius, we witness a change in the morphology-radius relation: we see a decrease in the fraction of late-type ($\sim$Sc) spiral galaxies with smaller cluster-centric radii. We also see some indication of a decrease in the early-type spirals. It is interesting to note that the critical density of $\sim 1\,h_{75}^{-2}\,\mathrm{Mpc}^{-2}$ seen in the SFR-density relation of Gómez et al. corresponds to a cluster-centric radius of between ~ 1 to 2 virial radii. The key question is: Are these two phenomena just different manifestations of the same physical process that is transforming both the morphology and the SFR of the galaxies at this critical density? I believe the jury is still out on this question.

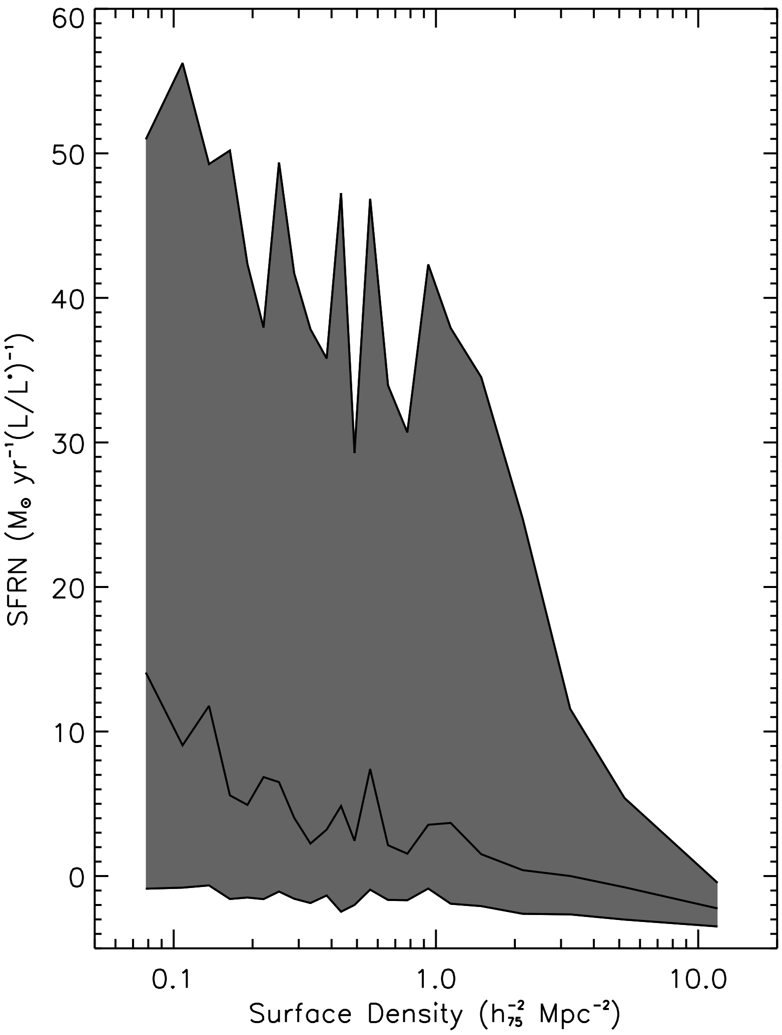

Fig. 1.8. The relation between SFR and density for a volume-limited sample of 8598 SDSS galaxies within $0.05 < z < 0.095$. The y-axis is the normalized SFR, i.e. the SFR divided by the z luminosity of the galaxy. The x-axis is the projected local surface density computed from the distance to the $10^{\rm th}$ nearest neighbor in a redshift shell of $\pm 1000\,{\rm km\,s^{-1}}$. See Gómez et al. (2003) for details. The top of the shaded region is the $75^{\rm th}$ percentile of the distribution, while the bottom is the $25^{\rm th}$ percentile. The solid line through the shaded area is the median of the distribution. As one can see, beyond a density of $\sim 1\,h_{75}^{-2}\,{\rm Mpc^{-2}}$, the tail of the distribution ($75^{\rm th}$ percentile) is heavily curtailed in dense environments.

I note here that Postman & Geller (1984) also reported a critical density (or "break") in their morphology-density relation at approximately the same density as seen in Figure 1.8, i.e. $\sim 3.5 h_{75}^{-3}\,{\rm Mpc^{-3}}$. Therefore, this "break" (or critical density) seen in the morphology-density relation appears to be universal, as it has been seen in two separate studies, which are based on different selection criteria and analysis techniques.

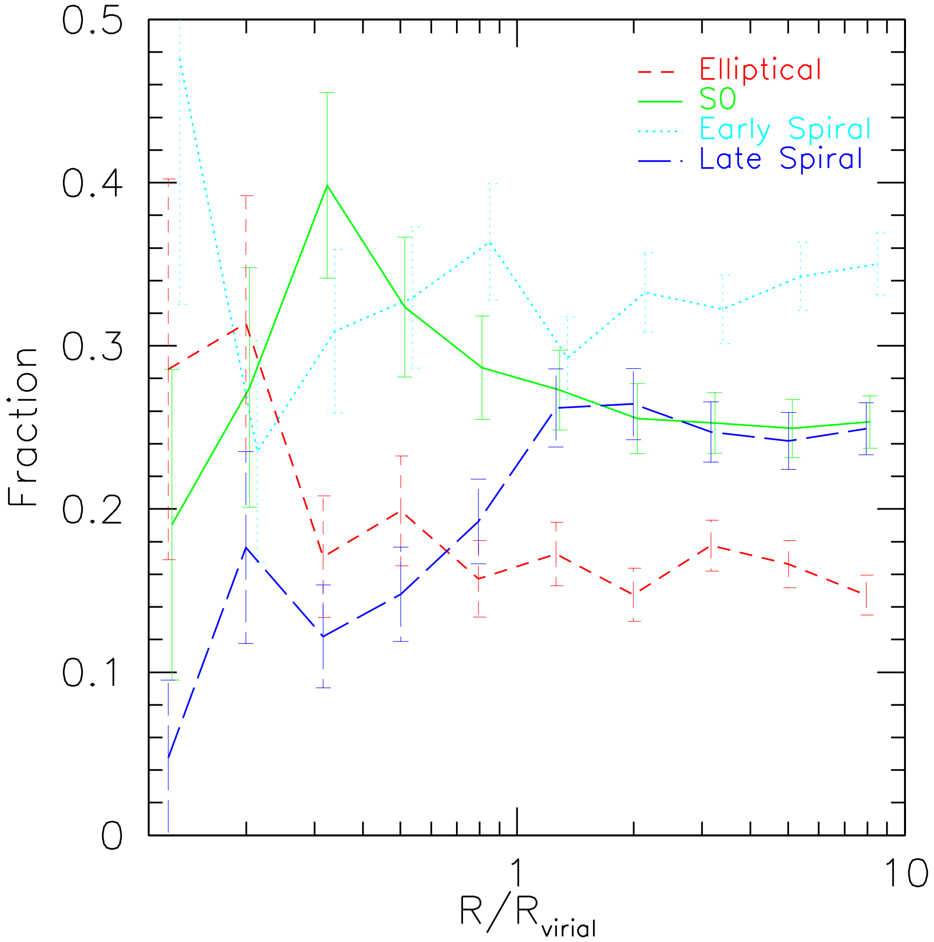

Fig. 1.9. The morphology-radius relation for C4 clusters in the SDSS. The morphologies were derived using the T_{auto} parameter discussed in the text, while the distance to the nearest C4 cluster (x-axis) has been scaled by the virial radius of that clusters. These plots were adapted from Gómez et al. (2003) and Goto et al. (2004).

1.6 Strangulation of Star Formation

One possible physical model* for explaining the critical density seen at $\sim 1 h_{75}^{-2}\,\mathrm{Mpc}^{-2}$ (or > 1 virial radius) in the SFR-density and morphology-radius relations is the stripping of the warm gas in the outer halo of infalling spiral galaxies via tidal interactions with the cluster potential. This process removes the reservoir of hydrogen that replenishes the gas in the cold disk of the galaxy, and thus slowly strangles (or starves) the star formation in the disk, leading to a slow death (see Larson, Tinsley, & Caldwell 1980; Balogh, Navarro, & Morris 2000; Diaferio et al. 2001). Recent *N*-body simulations of this model by Bekki, Shioya,

* See the reviews of Bower, Mihos, and Moore in this volume for a discussion of other physical mechanisms that can affect the properties of galaxies in clusters and groups of galaxies.

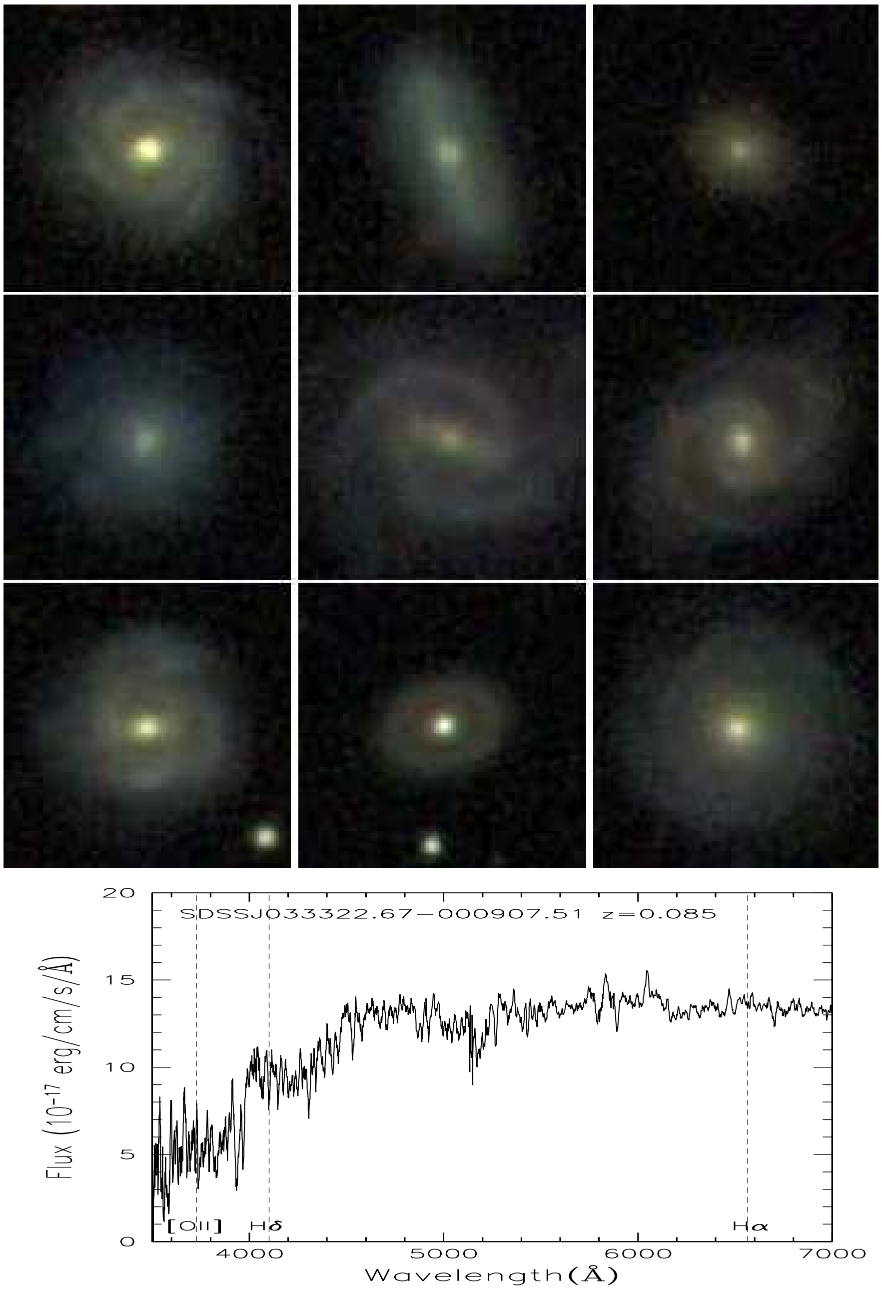

Fig. 1.10. *Top*: Nine images of "passive" spiral galaxies found by Goto et al. (2003) in their search for anemic galaxies in the SDSS database. Note the lack of "blue" H II, star-forming regions in the arms of these spirals. *Bottom*: The SDSS spectrum for one of these "passive" spirals (the galaxy in the top left-hand corner). Notice the lack of any emission lines indicative of ongoing star formation. These plots were taken from Goto et al. (2003).

& Couch (2002) demonstrate that it is viable and can happen at large cluster radii (or low densities).

One possible observational consequence of this strangulation of star formation is the existence of red or passive spiral galaxies, those that possess a spiral morphology but have no observed ongoing star formation. Such galaxies have been found already in studies of high-redshift clusters of galaxies (Couch et al. 1998) and have been known for some time at low redshift as "anemic" spirals (see van den Bergh 1991), although their true nature has been debated by many (see Bothun & Sullivan 1980; Guiderdoni 1987). Goto et al. (2003) has performed an automated searched for such "passive" or "anemic" spirals within the SDSS database by looking for galaxies with a high $C_{\rm in}$ value (indicating a face-on spiral galaxy; see Shimasaku et al. 2001) but with no detected emission lines in their SDSS spectra. In total, they found 73 such galaxies, which comprises only $0.28\%\pm0.03\%$ of all spiral galaxies with the same $C_{\rm in}$ parameter values but with detected emission lines. I show some examples of these "passive" spirals in Figure 1.10.

The most interesting discovery of Goto et al. (2003) is the distribution of local densities for these "passive" spirals, which peaks at $\sim 1h_{75}^{-2}\,{\rm Mpc}^{-2}$. Therefore, these galaxies appear to be preferential located close to the critical density discussed above for the SFR-density and morphology-radius relations, i.e. in the infall regions of C4 clusters. This is consistent with the observed decrease in the late-type (Sc) spiral galaxies witnessed in Figure 1.9.

In summary, the quality and quantity of the SDSS data allow us to study the environmental dependences of galaxy properties in greater detail than before. There does appear to be at least one critical density (at $\sim 1h_{75}^{-2}\,{\rm Mpc}^{-2}$) affecting the properties of galaxies, and this could be due to the slow strangulation of star formation in these spiral galaxies as they fall into denser environments.

Acknowledgements. I would like to acknowledge the organizers of the conference for their invitation to participate and their hospitality in Pasadena. I also thank all my collaborators for allowing me to show their results and figures in this review. These include Chris Miller, Daniel Eisenstein, Risa Wechsler, Gus Evrard, Tim McKay, Tomo Goto, Michael Balogh, Ann Zabludoff, and my colleagues from both the SDSS-2dF LRG survey and SDSS. I thank Kathy Romer and Chris Miller for reading an earlier draft of this review.

Funding for the creation and distribution of the SDSS Archive has been provided by the Alfred P. Sloan Foundation, the Participating Institutions, the National Aeronautics and Space Administration, the National Science Foundation, the U.S. Department of Energy, the Japanese Monbukagakusho, and the Max Planck Society. The SDSS Web site is http://www.sdss.org/.

The SDSS is managed by the Astrophysical Research Consortium (ARC) for the Participating Institutions. The Participating Institutions are The University of Chicago, Fermilab, the Institute for Advanced Study, the Japan Participation Group, The Johns Hopkins University, Los Alamos National Laboratory, the Max-Planck-Institute for Astronomy (MPIA), the Max-Planck-Institute for Astrophysics (MPA), New Mexico State University, University of Pittsburgh, Princeton University, the United States Naval Observatory, and the University of Washington.

References

Annis, J., et al. 2004, in preparation
Bahcall, N. A., et al. 2003, ApJ, 585, 182
Balogh, M. L., Navarro, J. F., & Morris, S. L. 2000, ApJ, 540, 113
Beers, T. C., Flynn, K., & Gebhardt, K. 1990, AJ, 100, 32
Bekki, K., Shioya, Y., & Couch, W. J. 2002, ApJ, 577, 651
Benson, A. J., Baugh, C. M., Cole, S., Frenk, C. S., & Lacey, C. G. 2000, MNRAS, 316, 107
Berlind, A. A., et al. 2004, in preparation
Blanton, M. R., et al. 2001, AJ, 121, 2358
Blanton, M. R., Lin, H., Lupton, R. H., Maley, F. M., Young, N., Zehavi, I., & Loveday, J. 2003, AJ, 125, 2276
Böhringer, H., et al. 2001, A&A, 369, 826
Bothun, G. D., & Sullivan, W. T. 1980, ApJ, 242, 903
Bramel, D. A., Nichol, R. C., & Pope, A. C. 2000, ApJ, 533, 601
Collins, C. A., et al. 2000, MNRAS, 319, 939
Couch, W. J., Barger, A. J., Smail, I., Ellis, R. S., & Sharples, R. M. 1998, ApJ, 497, 188
Diaferio, A., Kauffmann, G., Balogh, M. L., White, S. D. M., Schade, D., & Ellingson, E. 2001, MNRAS, 323, 999
Dressler, A. 1980, ApJ, 236, 351
Dressler, A., et al. 1997, ApJ, 490, 577
Eisenstein, D. J. 2003, ApJ, 586, 718
Eisenstein, D. J., et al. 2001, AJ, 122, 2267
Evrard, A. E., et al. 2002, ApJ, 573, 7
Fukugita, M., Ichikawa, T., Gunn, J. E., Doi, M., Shimasaku, K., & Schneider, D. P. 1996, AJ, 111, 1748
Gladders, M. D., & Yee, H. K. C. 2000, AJ, 120, 2148
Gómez, P. L., et al. 2003, ApJ, 584, 210
Goto, T. et al. 2002, AJ, 123, 1807
——. 2003, PASJ, 55, 757
——. 2004, in preparation
Guiderdoni, B. 1987, A&A, 172, 27
Gunn, J. E., et al. 1998, AJ, 116, 3040
Hogg, D. W., et al. 2003, ApJ, 585, L5
Hogg, D. W., Finkbeiner, D. P., Schlegel, D. J., & Gunn, J. E. 2001, AJ, 122, 2129
Jenkins, A., Frenk, C. S., White, S. D. M., Colberg, J. M., Cole, S., Evrard, A. E., Couchman, H. M. P., & Yoshida, N. 2001, MNRAS, 321, 372
Kepner, J., Fan, X., Bahcall, N., Gunn, J., Lupton, R., & Xu, G. 1999, ApJ, 517, 78
Kim, R. S. J., et al. 2002, AJ, 123, 20
Kochanek, C. S., White, M., Huchra, J., Macri, L., Jarrett, T. H., Schneider, S. E., & Mader, J. 2003, ApJ, 585, 161
Larson, R. B., Tinsley, B. M., & Caldwell, C. N. 1980, ApJ, 237, 692
Lee, B., et al. 2004, ApJ, submitted
Lewis, I. J., et al. 2002, MNRAS, 334, 673
Lucey, J. R. 1983, MNRAS, 204, 33
Lupton, R. H., Gunn, J. E., Ivezić, Z., Knapp, G. R., Kent, S., & Yasuda, N. 2001, in Astronomical Data Analysis Software and Systems X, ed. F. R. Harnden, Jr., F. A. Primini, & H. E. Payne (San Francisco: ASP), 269
Miller, C. J. 2000, Ph.D. Thesis, Univ. of Maine
Miller, C. J., et al. 2001, AJ, 122, 3492
Nichol, R. C. 2002, in Tracing Cosmic Evolution with Galaxy Clusters, ed. S. Borgani, M. Marino, & G. Valdarini (San Francisco: ASP), 57
Nichol, R. C., et al. 2001, in Mining the Sky, ed. A. J. Banday, S. Zaroubi, & M. Bartelmann (Heidelberg: Springer-Verlag), 613
Nichol, R. C., Collins, C. A., Guzzo, L., & Lumsden, S. L. 1992, MNRAS, 255, 21P
Peacock, J. A., & Nicholson, D. 1991, MNRAS, 253, 307
Pier, J. R., Munn, J. A., Hindsley, R. B., Hennessy, G. S., Kent, S. M., Lupton, R. H., & Ivezić, Z. 2003, AJ, 125, 1559
Postman, M. 2002, in Tracing Cosmic Evolution with Galaxy Clusters, ed. S. Borgani, M. Marino, & G. Valdarini (San Francisco: ASP), 3
Postman, M., & Geller, M. J. 1984, ApJ, 281, 95
Postman, M., Huchra, J. P., & Geller, M. J. 1992, ApJ, 384, 404

Postman, M., Lubin, L. M., Gunn, J. E., Oke, J. B., Hoessel, J. G., Schneider, D. P., & Christensen, J. A. 1996, AJ, 111, 615
Schlegel, D. J., Finkbeiner, D. P., & Davis, M. 1998, ApJ, 500, 525
Shimasaku, K., et al. 2001, AJ, 122, 1238
Smith, J. A., et al. 2002, AJ, 123, 2121
Stoughton, C., et al. 2002, AJ, 123, 485 (erratum: 123, 3487)
Strauss, M. A., et al. 2002, AJ, 124, 1810
Sutherland, W. 1988, MNRAS, 234, 159
Treu, T., Ellis, R. S., Kneib, J.-P., Dressler, A., Smail, I., Czoske, O., Oemler, A., & Natarajan, P. 2003, ApJ, 591, 53
van den Bergh, S. 1991, PASP, 103, 390
Wechsler, R. H., et al. 2004, in preparation
Yamauchi, C., et al. 2004, in preparation
York, D. G., et al. 2000, AJ, 120, 1579
Zehavi, I., et al. 2002, ApJ, 571, 172